

Cancer-associated fibroblast-induced M2-polarized macrophages promote hepatocellular carcinoma progression via the plasminogen activator inhibitor-1 pathway

SHUHAI CHEN¹, YUJI MORINE^{1,2}, KAZUNORI TOKUDA¹, SHINICHIRO YAMADA¹,
YU SAITO¹, MASA AKI NISHI¹, TETSUYA IKEMOTO¹ and MITSUO SHIMADA¹

¹Department of Digestive and Transplant Surgery, Tokushima University; ²Department of Surgery, Institute of Biomedical Sciences, Tokushima University Graduate School, Tokushima 770-8503, Japan

Received December 28, 2020; Accepted April 22, 2021

DOI: 10.3892/ijo.2021.5239

Abstract. Targeting the tumor stroma is an important strategy in cancer treatment. Cancer-associated fibroblasts (CAFs) and tumor-associated macrophages (TAMs) are two main components in the tumor microenvironment (TME) in hepatocellular carcinoma (HCC), which can promote tumor progression. Plasminogen activator inhibitor-1 (PAI-1) upregulation in HCC is predictive of unfavorable tumor behavior and prognosis. However, the crosstalk between cancer cells, TAMs and CAFs, and the functions of PAI-1 in HCC remain to be fully investigated. In the present study, macrophage polarization and key paracrine factors were assessed during their interactions with CAFs and cancer cells. Cell proliferation, wound healing and Transwell and Matrigel assays were used to investigate the malignant behavior of HCC cells *in vitro*. It was found

that cancer cells and CAFs induced the M2 polarization of TAMs by upregulating the mRNA expression levels of CD163 and CD206, and downregulating IL-6 mRNA expression and secretion in the macrophages. Both TAMs derived from cancer cells and CAFs promoted HCC cell proliferation and invasion. Furthermore, PAI-1 expression was upregulated in TAMs after being stimulated with CAF-conditioned medium and promoted the malignant behavior of the HCC cells by mediating epithelial-mesenchymal transition. CAFs were the main producer of C-X-C motif chemokine ligand 12 (CXCL12) in the TME and CXCL12 contributed to the induction of PAI-1 secretion in TAMs. In conclusion, the results of the present study suggested that CAFs promoted the M2 polarization of macrophages and induced PAI-1 secretion via CXCL12. Furthermore, it was found that PAI-1 produced by the TAMs enhanced the malignant behavior of the HCC cells. Therefore, these factors may be targets for inhibiting the crosstalk between tumor cells, CAFs and TAMs.

Correspondence to: Dr Yuji Morine, Department of Surgery, Institute of Biomedical Sciences, Tokushima University Graduate School, 3-18-15 Kuramoto-cho, Tokushima 770-8503, Japan
E-mail: ymorine@tokushima-u.ac.jp

Abbreviations: ACTA2, actin α -2; CAFs, cancer-associated fibroblasts; CCK-8, Cell Counting Kit-8; CM, conditioned medium; CXCL12, C-X-C motif chemokine ligand 12; CXCR4, C-X-C motif chemokine receptor 4; EMT, epithelial-mesenchymal transition; ESCC, esophageal squamous cell carcinoma; FAP, fibroblast activation protein; HCC, hepatocellular carcinoma; HSCs, hepatic stellate cells; IHCC, intrahepatic cholangiocarcinoma; NRF2, nuclear factor erythroid 2-related factor 2; OSCC, oral squamous cell carcinoma; PAI-1, plasminogen activator inhibitor-1; PCa, prostate cancer; PDAC, pancreatic ductal adenocarcinoma; PMA, phorbol-12-myristate-13-acetate; RT-qPCR, reverse transcription-quantitative PCR; TAMs, tumor-associated macrophages; TME, tumor microenvironment; VEGF, vascular endothelial growth factor

Key words: tumor-associated macrophages, cancer-associated fibroblasts, hepatocellular carcinoma, plasminogen activator inhibitor-1, epithelial-mesenchymal transition

Introduction

Unsuccessful efforts to destroy tumors suggest that therapies focusing only on cancer cells are usually not sufficient to eradicate malignant tumors (1). Tumors are surrounded by several non-cancerous components, including fibroblasts, immune-cells, adipose cells, blood vessels composed of endothelial cells and pericytes, extracellular matrix, infiltrated nerves and a variety of soluble molecules, such as chemokines, interleukins, lactate and vascular endothelial growth factor (VEGF). These factors have been associated with tumor cells and form the tumor microenvironment (TME), which provides an essential foundation to support the growth, metabolic reprogramming, immunosuppressive abilities, metastasis, recurrence and treatment resistance of malignant tumors (2,3). In the past decade, an increasing number of studies have highlighted the importance of the interactions between the TME and tumor cells (4-6) and targeting the tumor stroma has emerged as a novel cancer treatment paradigm (3,4,7). However, the molecular mechanisms underlying the interactions between tumor cells and the TME are complicated and the interactions between different types of stromal cells in the TME remain unknown.

Hepatocellular carcinoma (HCC) is one of the most aggressive malignant tumors and has been associated with a high mortality rate worldwide (8). Cancer-associated fibroblasts (CAFs) and tumor-associated macrophages (TAMs) are the main stromal cells in the TME of HCC (9). Interactions between CAFs and TAMs have been reported to promote tumor progression in several types of cancer, such as prostate cancer (PCa) (4), pancreatic ductal adenocarcinoma (PDAC) (5), esophageal squamous cell carcinoma (ESCC) (10), neuroblastoma (11), intrahepatic cholangiocarcinoma (IHCC) (12), breast cancer (13) and oral squamous cell carcinoma (OSCC) (14). In HCC, activated hepatic stellate cells (HSCs) can reprogram monocytes to acquire an immunosuppressive phenotype, thereby altering their paracrine factor environment to support the development of HCC (15). This suggested that CAFs could regulate tumor inflammation by modifying the presence and phenotype of invasive TAMs.

Plasminogen activator inhibitor-1 (PAI-1) is a serine protease inhibitor encoded by the serpin family E member 1 gene (16). PAI-1 was found to be upregulated in a variety of different tumors, such as breast (17), ovarian (18) and colon cancers (19), and possess several pro-tumorigenic functions, including supporting proliferation and angiogenesis, inhibiting cell apoptosis and promoting metastasis (17,18,20). Along with cancer cells, several other components of the TME, including platelets, macrophages and vascular cells, also secrete PAI-1 (16,21). In HCC, it has been observed that PAI-1 was upregulated and high PAI-1 protein expression level was predictive of unfavorable tumor behavior and prognosis (22). However, the biological roles of PAI-1 in the TME are yet to be fully elucidated.

The present study established an *in vitro* model, using the indirect contact coculture method to simulate the crosstalk between cancer cells, CAFs and TAMs. It was investigated whether CAFs could induce TAMs to adapt their polarization into a special phenotype and whether they could mediate their paracrine signaling to promote the malignant behavior of HCC. Furthermore, important factors involved in this process were investigated to provide evidence that inhibiting the crosstalk in the TME, by targeting these factors, may be beneficial for improving the prognosis of patients with HCC.

Materials and methods

Cell culturing and reagents. The human HCC cell line, Huh-7 (RIKEN BioResource Research Centre) and the human HSC line, Lx-2 (Merck KGaA) were cultured in DMEM, supplemented with 10% FBS and a 1% penicillin-streptomycin solution (all from Thermo Fisher Scientific, Inc.). The human monocyte cell line, THP-1, was obtained from the Japanese Collection of Research Bioresources Cell Bank and was cultured in RPMI-1640 medium, supplemented with 10% FBS and a 1% penicillin-streptomycin solution (all from Thermo Fisher Scientific, Inc.). All experiments were performed with mycoplasma-free cells. The cells were cultured at 37°C in a humidified incubator with 5% CO₂ and were selected for experiments in the logarithmic growth phase.

To induce the M0 macrophages (M0), the THP-1 cells were treated with 150 nM phorbol-12-myristate-13-acetate (PMA; Sigma-Aldrich; Merck KGaA) for 48 h at 37°C. The human

C-X-C motif chemokine 12 (CXCL12) antibody (300 µg/ml; cat. no. AF-310-NA), normal human IgG control (300 µg/ml; cat. no. 1-001-A) and recombinant human PAI-1 (rPAI-1; 100 ng/ml; cat. no. 1786-PI) were purchased from R&D Systems, Inc. Tiplaxtinin (PAI-039; a selective PAI-1 inhibitor; cat. no. s7922) was purchased from Selleck Chemicals.

Preparation of conditioned medium (CM). The Huh-7 and Lx-2 cells, and M0 were cultured to 80% confluency, washed twice with PBS, then incubated with DMEM containing 1% FBS for 48 h at 37°C. The supernatant was collected, centrifuged (500 x g; 20 min) at room temperature and filtered using a 0.2-µm filter to remove the cell debris. The CM was stored at -80°C, and repeated freeze-thaw cycles were avoided. For treating the indicated cells, the CM was added to the complete growth medium at a ratio of 1:2, and the cells were stimulated for 48 h at 37°C. The Lx-2 cell line was treated with Huh-7-derived CM to obtain CAF(Ca), while M0 was treated with Huh-7-derived CM to obtain TAM(Ca). Next, M0 was treated with CAF(Ca)-derived CM and TAM(Ca)-derived CM to obtain TAM(CAF) and TAM(TAM), respectively (Fig. 1A). Then, the CM from M0, TAM(Ca), TAM(CAF) were further collected in the same manner as aforementioned and was added to the complete growth medium at a ratio of 1:2 for the next experiment.

For the PAI-1 inhibition experiment, 20 µM tiplaxtinin was added into normal DMEM, M0-CM, TAM(Ca)-CM and TAM(CAF)-CM. To determine the direct effects of PAI-1, 100 ng/ml rPAI-1 was added into normal DMEM (control). These CM were used to perform the cell proliferation, colony formation, wound healing, migration and invasion assays.

For the CXCL12 neutralization experiment, 300 µg/ml CXCL12 antibody or IgG control was added into the CAF-CM, which was subsequently used to stimulate M0 to obtain TAM(CAF + CXCL12 Ab) and TAM(CAF + IgG Ab), respectively (Fig. 1B).

Morphology analysis. For H&E staining, M0, TAM(Ca), TAM(CAF) and TAM(TAM) were seeded in the Nunc Lab-Tek II Chamber Slide system (cat. no. 154526PK; Thermo Fisher Scientific, Inc.). The subsequent steps were all performed at room temperature. The slides were gently washed twice with PBS and fixed with 90% ethanol for 15 min. Then, the slides were stained with hematoxylin (Muto Pure Chemicals Co., Ltd.) for 10 min, washed under running water for 5 min and stained with eosin Y (FUJIFILM Wako Pure Chemical Corporation) for 5 min. After washing under running water for 5 min to remove the excess dye, the slides were sealed with a coverslip and neutral resin. Differences between each group were compared under a light microscope (magnification, x200).

Cell proliferation assay. The tumor cells were seeded at a density of 2x10⁴ cells/well into 96-well plates in complete medium and cultured in an incubator at 37°C. After adhesion, the cells were washed with PBS and cultured with the indicated CM at 37°C and the proliferative state of the cells was observed every 24 h between days 1 and 4. The Cell Counting Kit-8 (CCK-8) solution (Dojindo Molecular Technologies, Inc.) was added to the medium, as a 10% volume, and cell proliferation

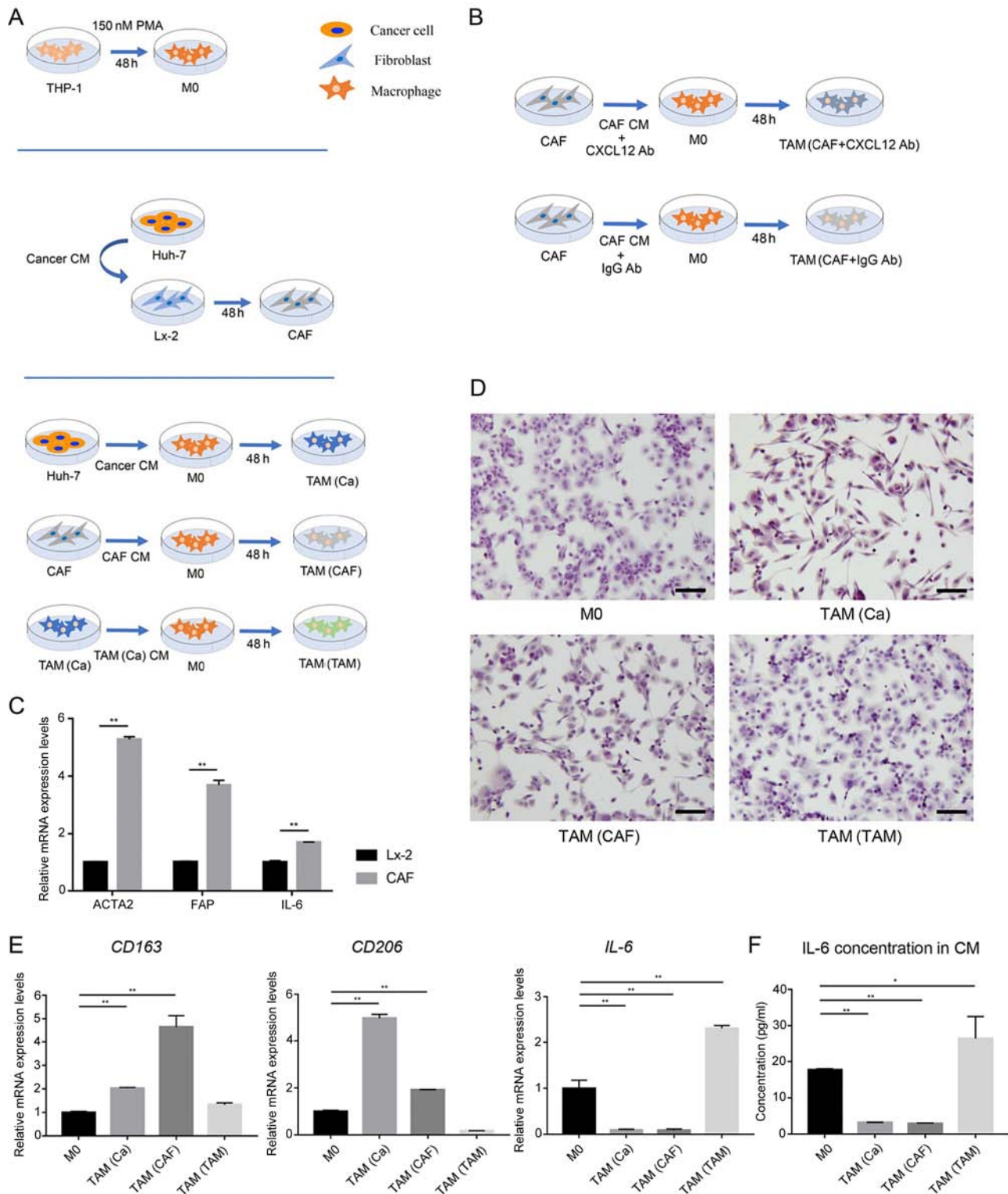


Figure 1. Cancer cells and CAFs induce M2 polarization in human macrophages. (A) Schematic representation of the generation of M0, CAFs and the three types of TAMs. (B) Schematic representation of anti-CXCL12 treatment in CAF-induced TAMs. (C) After treatment with CM from the Huh-7 cells, the gene expression levels of the CAFs markers were detected in the Lx-2 cells using RT-qPCR analysis. (D) Typical morphological changes in the M0 macrophages and different types of TAMs are shown following staining with H&E. Scale bar, 100 μ m. (E) Gene expression levels of M2-polarized macrophage markers were detected in M0 macrophages and different types of TAMs using RT-qPCR analysis. (F) Secretion of IL-6 in the CM of M0 and different types of TAMs. * $P < 0.05$; ** $P < 0.01$. CAF, cancer-associated fibroblast; CM, conditioned medium; RT-qPCR, reverse transcription-quantitative PCR; TAM, tumor-associated macrophage; PMA, phorbol-12-myristate-13-acetate; M0, macrophages; FAP, fibroblast activation protein; ACTA2, actin α -2; CXCL12, C-X-C motif chemokine ligand 12; Ab, antibody.

was analyzed by measuring the absorbance values at 450 nm with a microplate reader (SpectraMax i3; Molecular Devices, LLC) after 2 h, according to the manufacturer's instructions.

Colony formation assay. The cancer cells were seeded at a density of 200 cells/well in 6-well plates containing culture medium, then the plates were placed in an incubator at 37°C.

After 3 days, the growth medium was removed and the indicated CM was added in each group. The cells were cultured for 14 days and the medium was changed every 5 days. At the endpoint, 4% paraformaldehyde and 0.1% crystal violet was used to fix and stain the cells for 20 min at room temperature, respectively. After washing with PBS, images of the cell colonies from the different groups were captured using a light microscope (magnification, x40; BX43F; Olympus Corporation) and counted. The colony was only counted if it contained >50 cells.

Wound healing assay. The cancer cells were seeded, at a density of 5×10^5 cells/well into 6-well plates, and once they formed a confluent monolayer at 90%, a 200- μ l pipette tip was used to scratch a wound through the entire center of the well. After washing with PBS, the cells were cultured with indicated CM in the absence of FBS in each group for 12 h at 37°C. The areas of the wounds were observed, and images were captured using a light microscope (magnification, x40; DP22-CU; Olympus Corporation) at 0 h and 12 h after scratching. The cell migration rates were calculated using ImageJ v1.46r software (National Institutes of Health) and using the following equation: Relative migration rate=[width (0 h)-width (12 h)]/width (0 h) x100%.

Migration and invasion assays. A 24-well Transwell system, with 8.0- μ m pores (Corning, Inc.) was used for the migration and invasion assays. Serum-starved cancer cells were resuspended, adjusted to a concentration of 2×10^5 /ml, then seeded into the upper chamber, with 100- μ l cell suspension per well. Following cell attachment, the culture medium was changed to indicated CM in each group. The FBS concentration was 5% in the upper chambers and 10% in the lower chambers. After incubation for 24 h for migration assay and 36 h for invasion assay at 37°C, the upper chambers were fixed with 100% methanol for 20 min and stained with 0.1% crystal violet for 20 min, both at room temperature, following which the non-migrated cells on the upper chambers were removed using a cotton swab. The number of remaining cells was calculated and quantified in 5 random fields of view under a light microscopic (magnification, x100). For the invasion assays, the upper chambers of the Transwell system were precoated with Matrigel (Corning, Inc.) overnight at 37°C.

Cytokine array. A Human XL Cytokine Array kit (cat. no. ARY022B; R&D Systems, Inc.) was used to detect molecules in the CM from the Huh-7, Lx-2, CAF(Ca), M0, TAM(Ca) and TAM(CAF) cells, according to the manufacturer's instructions. Briefly, after blocking with Array Buffer 6 (2 ml for one membrane) for 1 h at room temperature, the membrane containing 105 different capture antibodies was incubated overnight with 400 μ l indicated CM at 4°C in each group. The following day, the membranes were washed with 1X Wash Buffer (diluted 1:25 with distilled water from Wash Buffer Concentrate) and incubated with the detection antibody cocktail and streptavidin-HRP in sequence. Finally, the membranes were treated with a chemiluminescent detection reagent for 1 min at room temperature and an Amersham Imager 600 (Cytiva) was used to detect the signal intensities on each membrane. Each pair of positive dots represented

the signals of highly expressed molecules and the luminescence intensity was quantified using ImageJ v1.46r software (National Institutes of Health). The full list of all the antibodies is available in the product datasheet.

ELISA. The Human IL-6 Quantikine ELISA kit (cat. no. D6050), Human Serpin E1/PAI-1 Quantikine ELISA kit (cat. no. DSE100) and Human CXCL12/stromal cell-derived factor 1 α Quantikine ELISA kit (cat. no. DSA00) were purchased from R&D Systems Inc., to detect the concentrations of IL-6, PAI-1 and CXCL12 in the CM, according to the manufacturer's instructions. The absorbance at 450 nm was measured using a microplate reader and 540 nm was set as the reference wavelength.

Reverse transcription-quantitative PCR (RT-qPCR). The total RNA, in each sample, was extracted using a RNeasy Mini kit (Qiagen GmbH), in accordance with the manufacturer's instructions, and a spectrophotometer (NanoDrop™ 2000; Thermo Fisher Scientific, Inc.) was used to measure and calculate the RNA concentration of the samples. Subsequently, 2.5 μ g RNA was reverse transcribed into cDNA, in a total 50 μ l reaction system, using a High-Capacity cDNA Reverse Transcription kit (Applied Biosystems; Thermo Fisher Scientific, Inc.) according to the manufacturer's instructions. Then, TaqMan qPCR was performed using a StepOnePlus Real-Time PCR system (Applied Biosystems; Thermo Fisher Scientific, Inc.). The following thermocycling conditions were used for qPCR: Initial denaturation at 95°C for 3 min, followed by 40 cycles of denaturation at 95°C for 30 sec, annealing at 58°C for 30 sec and extension at 72°C for 45 sec; and a final extension at 72°C for 10 min. The following TaqMan gene expression assays were used: ACTA2 (assay ID, Hs00426835_g1), CD163 (assay ID, Hs00174705_m1), CD206 (assay ID, Hs00267207_m1), E-cadherin (assay ID, Hs00170423_m1), N-cadherin (assay ID, Hs00169953_m1), CXCL12 (assay ID, Hs00930455_m1), CXCR4 (assay ID, Hs00976734_m1), FAP (assay ID, Hs00990791_m1), IL-6 (assay ID, Hs00985639_m1), PAI-1 (assay ID, Hs01126606_m1) (all from Thermo Fisher Scientific, Inc.). GAPDH (assay ID, 4326317E; Thermo Fisher Scientific, Inc.) was used as the internal control to normalize the raw data. Data analysis was performed using the $2^{-\Delta\Delta C_t}$ method for relative quantification (23) and the results are presented as the fold changes of the relative mRNA expression for each experimental group compared with that in the control group.

Western blot analysis. Total protein was extracted from the cell lines using freshly prepared RIPA lysis buffer (Thermo Fisher Scientific, Inc.), containing a protease inhibitor cocktail (Sigma-Aldrich; Merck KGaA) and a PhosSTOP phosphatase inhibitor cocktail (Roche Diagnostics). A BCA kit (Thermo Fisher Scientific Inc.) was used to measure the concentration of the protein. Equal amounts of protein (20 μ g) were separated on 12% (for Snail and Twist1) or 10% (for other proteins) SDS-PAGE and transferred onto PVDF membranes (Bio-Rad Laboratories, Inc.). To evaluate protein expression, the blots were blocked with 5% skimmed milk for 1 h at room temperature and incubated overnight at 4°C with the following primary antibodies: Anti-PAI-1 (1:1,000; cat. no. 11907; Cell Signaling

Technology, Inc.), anti-E-cadherin (1:1,000; cat. no. ab1416; Abcam), anti-N-cadherin (1:1,000; cat. no. 13116; Cell Signaling Technology, Inc.), anti-Snail family transcriptional repressor 1 (Snail; 1:1,000; cat. no. ab85936; Abcam), anti-Twist family bHLH transcription factor 1 (Twist1; 1:1,000; cat. no. SC-15393, Cosmo Bio Co., Ltd.) and anti- β -actin (1:2,000; cat. no. 4970; Cell Signaling Technology, Inc.). Then, anti-rabbit IgG, HRP-linked (1:2,000; cat. no. 7074; Cell Signaling Technology, Inc.) and anti-mouse IgG, HRP-linked (1:2,000; cat. no. 7076; Cell Signaling Technology, Inc.) were used as secondary antibodies, according to the species of the primary antibodies, for 1 h at room temperature. The proteins were detected with ECL reagents (Cytiva).

Statistical analysis. All the data are presented as the mean \pm SD. Statistical analysis and construction of the graphs was performed using GraphPad Prism v7.0 software (GraphPad Software, Inc.) and ImageJ v1.46r software (National Institutes of Health). Comparisons between two groups were evaluated using an unpaired Student's t-test or a Mann-Whitney U test. Differences among multiple groups were analyzed using one-way ANOVA followed by Tukey's post hoc test. All the experiments were repeated ≥ 3 times. $P < 0.05$ (two-sided) was considered to indicate a statistically significant difference.

Results

Cancer cells and CAFs induce M2 polarization in human macrophages. The THP-1 cells were treated with PMA for 48 h to induce their differentiation into M0 (Fig. 1A), as previously reported (24). CM from the HCC cells was used to stimulate the human HSC line, Lx-2 for 48 h. After activation by the cancer cells, the CAF markers, actin α -2 (*ACTA2*), fibroblast activation protein (*FAP*) and *IL-6* were markedly upregulated in the Lx-2 cells, indicating that the HSCs transdifferentiated into CAFs (Fig. 1C).

To mimic the crosstalk between tumor cells, CAFs and TAMs in the TME, the THP-1-induced M0 were treated with cancer cell-derived CM, CAF-derived CM and cancer cell-pretreated M0 macrophage-derived CM to obtain TAM(Ca), TAM(CAF) and TAM(TAM), respectively (Fig. 1A). Macrophage polarization is characterized by distinct morphological features (25). Using H&E staining, it was identified that TAM(Ca) and TAM(CAF) exhibited an elongated morphology, which was similar to that of M2-polarized macrophages. However, TAM(TAM) were predominantly round and more closely resembled M1-polarized macrophages (Fig. 1D).

Subsequently, the mRNA expression levels and the concentration of M2 polarization-related markers were measured using RT-qPCR and ELISA, respectively. TAM(Ca) and TAM(CAF) exhibited increased mRNA expression levels of *CD163* and *CD206*. In addition, the concentration of the M1 polarization-related marker, *IL-6* was decreased compared with that in the M0, confirming the M2 polarization of the macrophages. However, TAM(TAM) failed to express the M2 polarization-related markers and *IL-6* was upregulated at both the gene and protein levels (Fig. 1E and F). Therefore, the current study focused on TAM(Ca) and TAM(CAF) in the subsequent experiments.

TAM(Ca) and TAM(CAF) promote HCC cell malignant behavior in vitro. To investigate the effects of different types of TAMs on the HCC cells, Huh-7 was treated with CM collected from M0, TAM(Ca) and TAM(CAF), and normal culture medium was used as control. The CCK-8 assay results demonstrated that after 4 days of culture, the M0 did not increase the proliferation of the Huh-7 cells compared with that in the control group, while the TAM(Ca) and TAM(CAF) groups significantly promoted the proliferation of the Huh-7 cells compared with that in the M0 and normal medium control groups. However, there was no significant difference between the TAM(Ca) and TAM(CAF) groups (Fig. 2A). Similar results were obtained from the colony formation assays, which revealed that the TAM(Ca) and TAM(CAF) experimental groups significantly promoted the colony formation of Huh-7 cells compared with that in the M0 group (Fig. 2B). Furthermore, compared with that in the M0, TAM(Ca) and TAM(CAF) significantly promoted the migration of the Huh-7 cells, as detected in the wound healing (Fig. 2C) and Transwell (Fig. 2D) assays. The Matrigel assay results identified that the invasive ability of the Huh-7 cells was also enhanced by the two types of TAMs (Fig. 2E). Collectively, these results suggested that both TAM(Ca) and TAM(CAF) promoted HCC cell proliferation, migration and invasion *in vitro*.

PAI-1 expression is upregulated in CAF-induced TAMs compared with that in the cancer cell-induced TAMs. To further investigate the interactions between CAFs and TAMs, the factors secreted by TAM(Ca) and TAM(CAF) were compared. According to the results of the cytokine array, several factors, such as PAI-1, *IL-8*, platelet derived growth factor-AA (PDGF-AA) and T-cell immunoglobulin mucin 3 (TIM-3) were upregulated in the CM from the M0 after stimulation with the CM from cancer cells and CAFs (Fig. 3A). In addition, a total of 7 factors with notable differences in secretion between the TAM(Ca) and TAM(CAF) were selected and quantified (Fig. 3B). Among these, PAI-1 exhibited the highest fold change. The western blot analysis and ELISA results demonstrated that TAM(CAF) expressed higher protein expression levels and released higher concentrations of PAI-1, respectively, compared with that in the TAM(Ca) and M0 (Fig. 3C and D). The Huh-7 cells also secreted PAI-1; however, the concentration of PAI-1 in the CM of TAM(CAF) was significantly higher compared with that in the Huh-7 cells (Fig. 3D).

Accumulating evidence has suggested that PAI-1 contributed to tumor cell proliferation, migration, invasion, drug resistance and epithelial-mesenchymal transition (EMT), and that high PAI-1 protein expression was associated with unfavorable biological behavior and patient prognosis in HCC (19,21,22). Therefore, the present study selected PAI-1 for subsequent functional analysis and investigated the roles of PAI-1 in TAM(CAF).

Inhibition of PAI-1 suppresses the tumor-promoting effects of TAM(CAF) in vitro. To evaluate the functions of PAI-1 in the tumors cells, the functional activity of PAI-1 in the CM of TAM(CAF) was inhibited using tiplaxtinin, a small-molecule specific inhibitor of PAI-1 (26). First, the effect of tiplaxtinin on

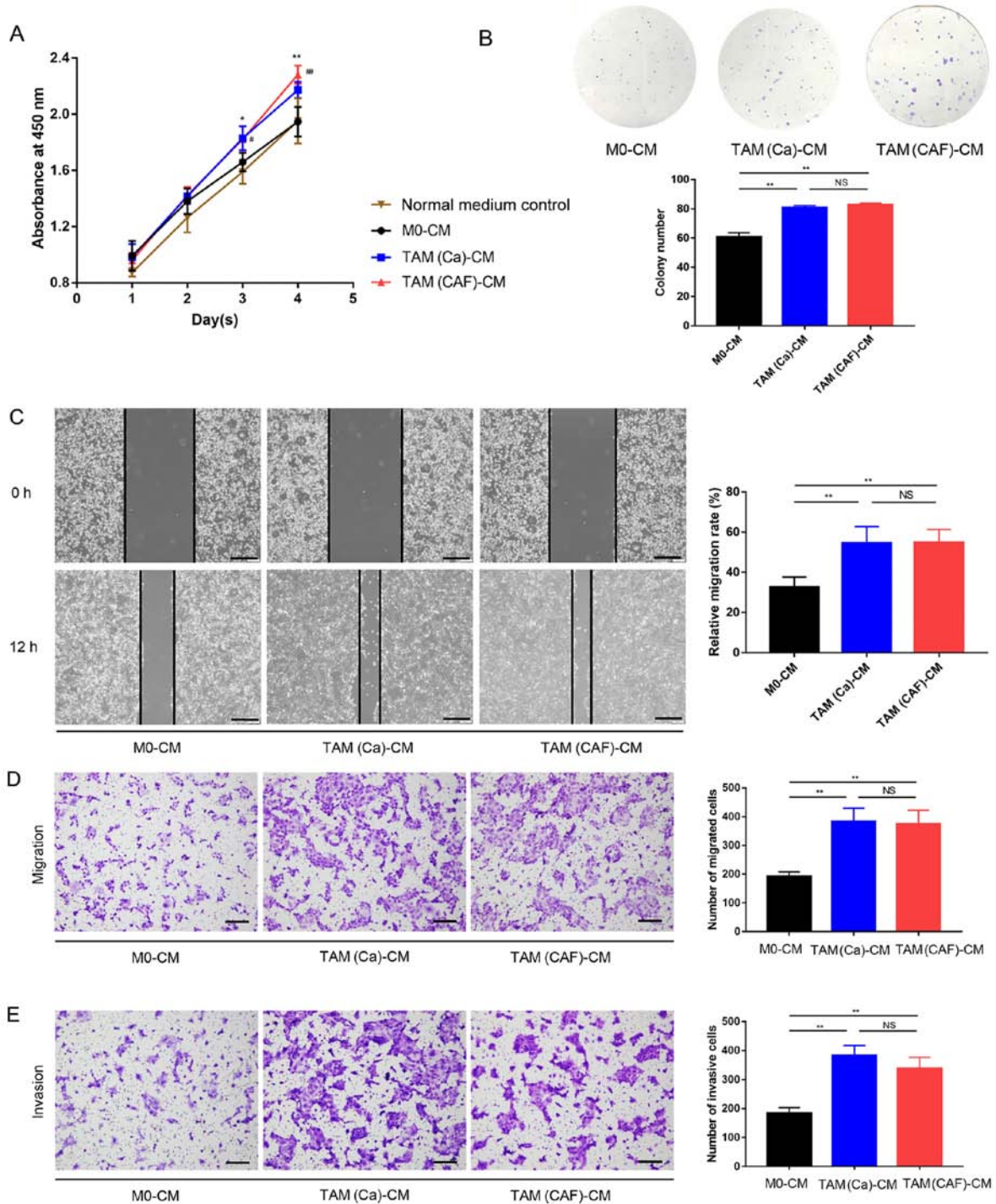


Figure 2. TAM(Ca) and TAM(CAF) promote HCC cell malignant behavior *in vitro*. (A) Cell Counting Kit-8 and (B) colony formation assay results demonstrated the effect of different types of TAMs on the proliferation of the Huh-7 cells. * $P < 0.05$, ** $P < 0.01$, # $P < 0.05$ and ## $P < 0.01$ vs. M0-CM. (C) Wound healing (scale bar, 400 μm) and (D) Transwell and (E) Matrigel assays (scale bar, 200 μm) indicated that TAM(Ca) and TAM(CAF) promoted Huh-7 cell migration and invasion compared with that in the M0. ** $P < 0.01$. CAF, cancer-associated fibroblast; TAM, tumor-associated macrophage; CM, conditioned medium; M0, macrophages; NS, not significant.

the proliferation of the Huh-7 cell line was determined. As the data showed, tiplaxtinin at 20 μM had no effect on proliferation (Fig. 3E). The data from the CCK-8 and colony formation assays demonstrated that the proliferation-promoting effect of TAM(CAF), but not TAM(Ca) or M0, was impaired following the inhibition of PAI-1 (Fig. 3E and F). These results indicated that the decreased proliferation was due to the inhibition of PAI-1 function rather than the direct cytotoxic effects of

tiplaxtinin. In addition, following the inhibition of PAI-1, the migratory and invasive abilities of the HCC cells were significantly decreased in the TAM(CAF) group compared with that in the TAM(CAF) group without tiplaxtinin (Fig. 3G-I). It was also found that treatment with rPAI-1 directly increased the malignancy of the HCC cells (Fig. 4A-D). Mechanistically, the downregulation of E-cadherin and upregulation of N-cadherin, Snail and Twist1 revealed that TAM(Ca) and TAM(CAF)

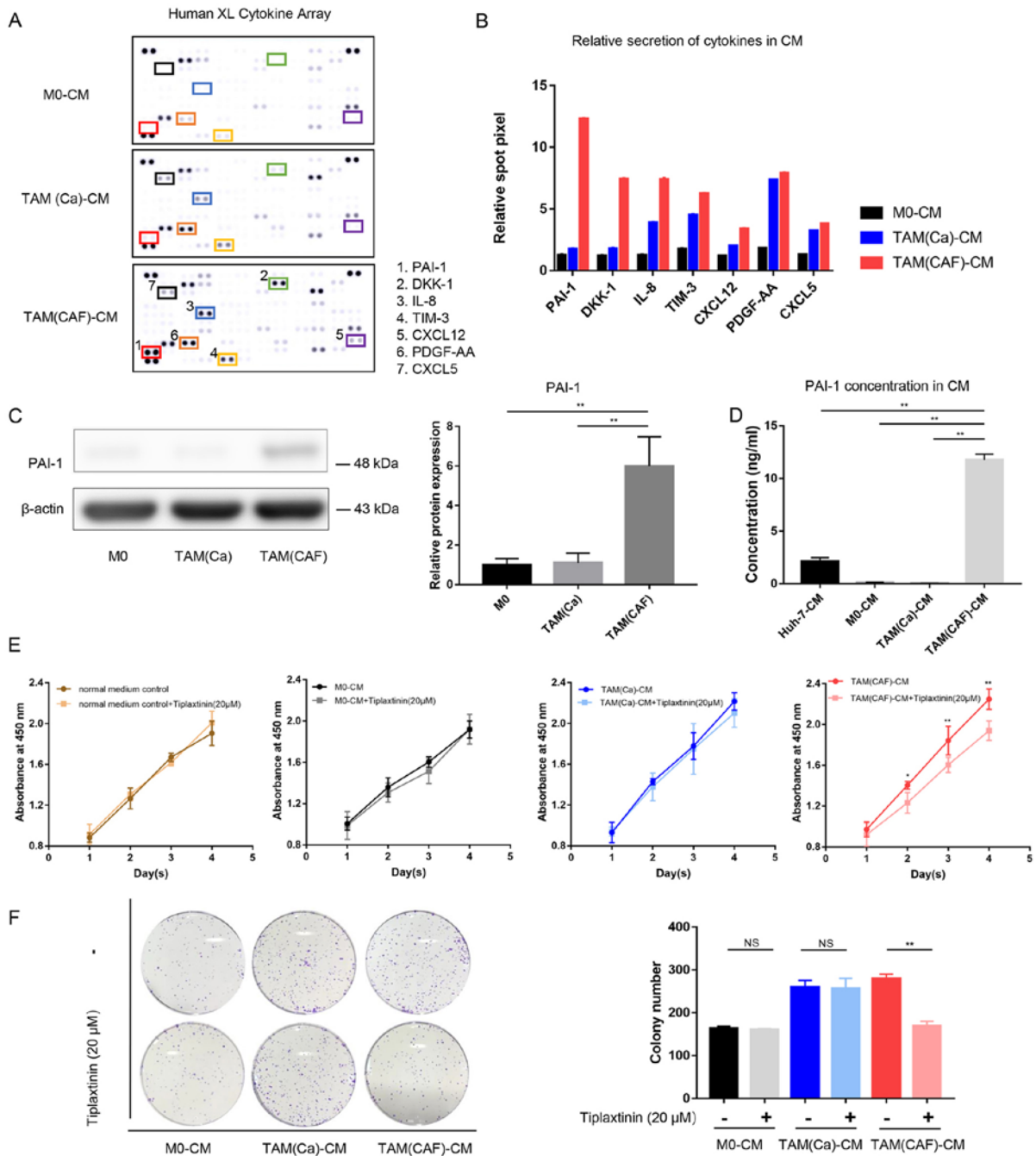


Figure 3. Continued.

promoted EMT in the cancer cells compared with that in the M0 group, while PAI-1 inhibition diminished this effect in the TAM(CAF) group (Fig. 4E and F). Taken together, these results suggested that TAM(CAF)-secreted PAI-1 contributed to the malignant behavior of the HCC cells by mediating EMT.

CAF-derived CXCL12 contributes to the secretion of PAI-1 in TAM(CAF). As the aforementioned results suggested a significant role of PAI-1 in tumor-promoting processes, the mechanisms underlying the specific secretion of PAI-1 in TAM(CAF) was further investigated. The differences in the factors between the CM from the Huh-7 cells and the CAFs were compared (Fig. 5A). The results of the cytokine array indicated that the levels of CXCL12 and C-C motif chemokine ligand 5

were markedly higher in the CM from the CAFs compared with that in the CM from the cancer cells (Fig. 5B). As CXCL12 is known to promote the transcription and secretion of PAI-1 (27), CXCL12 was selected for subsequent analysis.

The RT-qPCR and ELISA results demonstrated that the CAFs had higher mRNA expression level and secreted more CXCL12 compared with that in the normal fibroblasts, and these were the primary source of CXCL12 in the TME (Fig. 5C and D). Next, the mRNA expression level of C-X-C motif chemokine receptor 4 (*CXCR4*), which is the receptor of CXCL12 (28), was measured in the M0, TAM(Ca) and TAM(CAF). Consistent with the current hypothesis, it was found that TAM(CAF) overexpressed the *CXCR4* gene (Fig. 5E). Furthermore, CXCL12 neutralization with a CXCL12 antibody

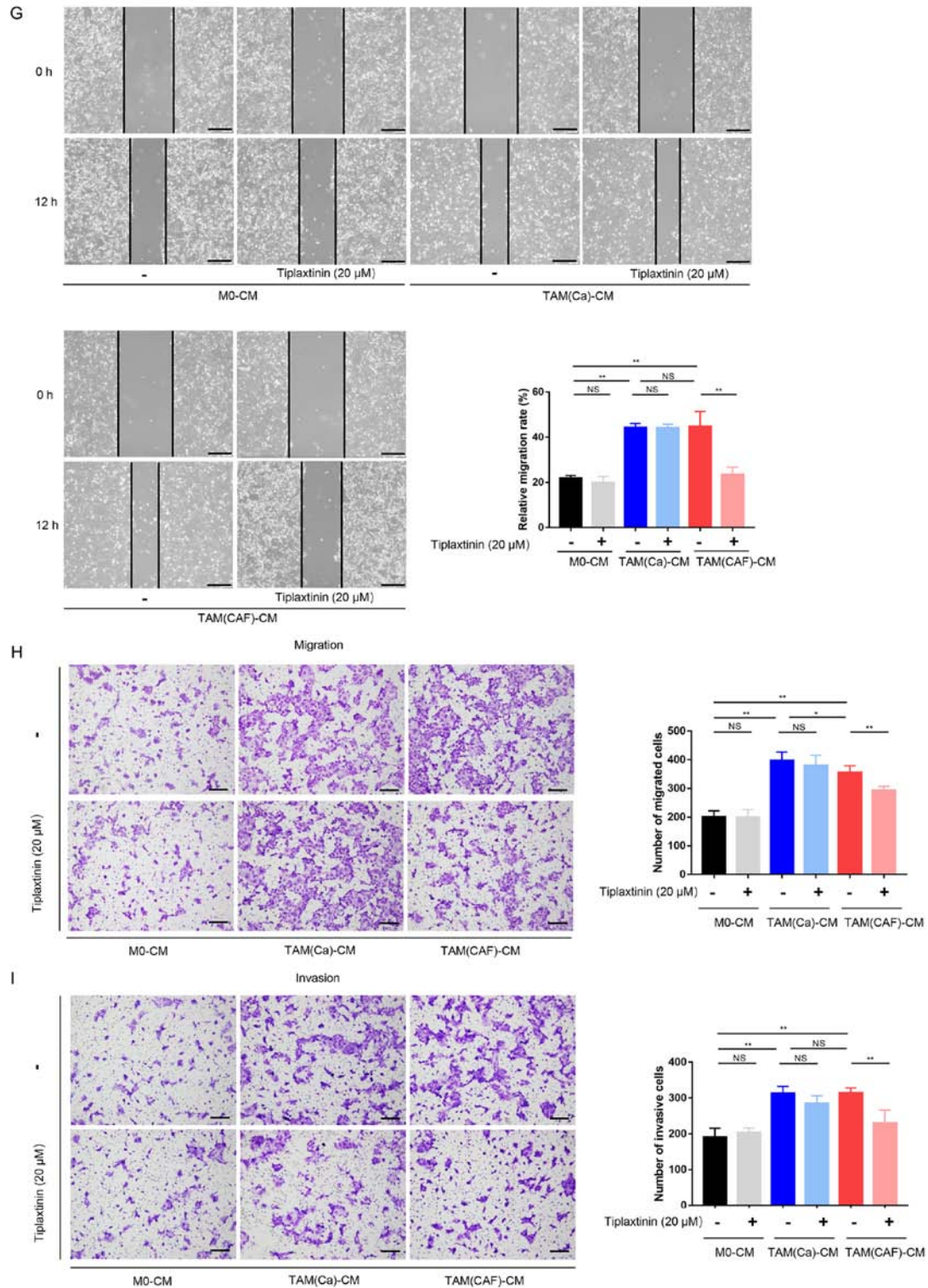


Figure 3. PAI-1 is the key factor secreted by TAMs following CAF-CM stimulation and promotes tumor malignant behavior *in vitro*. (A) Original image and (B) spot pixel value from a cytokine array revealed the profiles of paracrine factors in the M0-CM, TAM (Ca)-CM and TAM(CAF)-CM. (C) Western blot and (D) ELISA results indicated that PAI-1 was upregulated in the TAM(CAF) group compared with that in the M0 and TAM(Ca) groups. (E) Cell Counting Kit-8 and (F) colony formation assays showed that the inhibition of PAI-1 in TAM(CAF)-CM suppressed the enhanced proliferation of Huh-7 cells. (G) Wound healing (scale bar, 400 μm) and (H) Transwell and (I) Matrigel (scale bar, 200 μm) assays indicated that the inhibition of PAI-1 in the TAM(CAF)-CM group suppressed the enhanced migration and invasion of the Huh-7 cells. *P<0.05; **P<0.01. CAF, cancer-associated fibroblast; CM, conditioned medium; CXCL12, C-X-C motif chemokine ligand 12; CXCL5, C-X-C motif chemokine ligand 5; PAI-1, plasminogen activator inhibitor-1; PDGF-AA, platelet derived growth factor-AA; TAM, tumor-associated macrophage; TIM-3, T-cell immunoglobulin mucin 3; M0, macrophages; NS, not significant.

in the CM of CAFs reduced the mRNA expression level and the secretion of PAI-1 in the TAM(CAF) (Figs. 1B and 5F and G), suggesting that CXCL12 could be an inducer of PAI-1 secretion

in TAM(CAF). Collectively, these results indicated that the HCC cells induced the transformation of HSCs into CAFs and upregulated the expression level of CXCL12. Through various

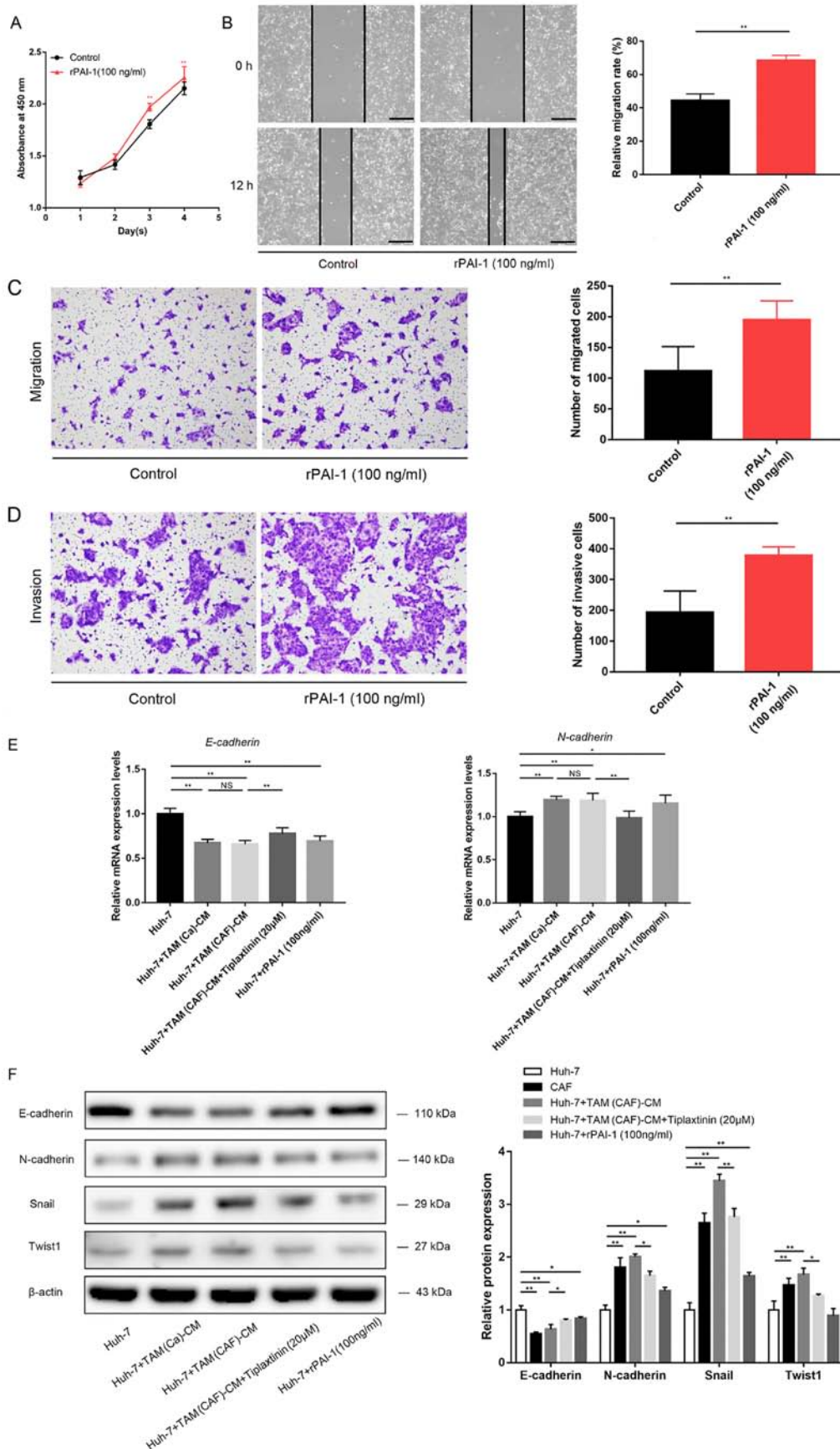


Figure 4. PAI-1 promotes HCC malignant behavior by mediating EMT. (A) Cell Counting Kit-8, (B) wound healing (scale bar, 400 μ m), (C) Transwell and (D) Matrigel (scale bar, 200 μ m) assays demonstrated the direct effects of PAI-1 on tumor cell malignant behavior. (E) EMT-related gene expression was detected using reverse transcription-quantitative PCR in the Huh-7 cells. (F) Western blot analysis revealed the protein expression levels of E-cadherin, N-cadherin, Snail and Twist1 in the Huh-7 cells under the specified treatment conditions. * $P < 0.05$; ** $P < 0.01$. CAF, cancer-associated fibroblast; CM, conditioned medium; PAI-1, plasminogen activator inhibitor-1; Snail, snail family transcriptional repressor 1; TAM, tumor-associated macrophage; Twist1, twist family BHLH transcription factor 1; NS, not significant.

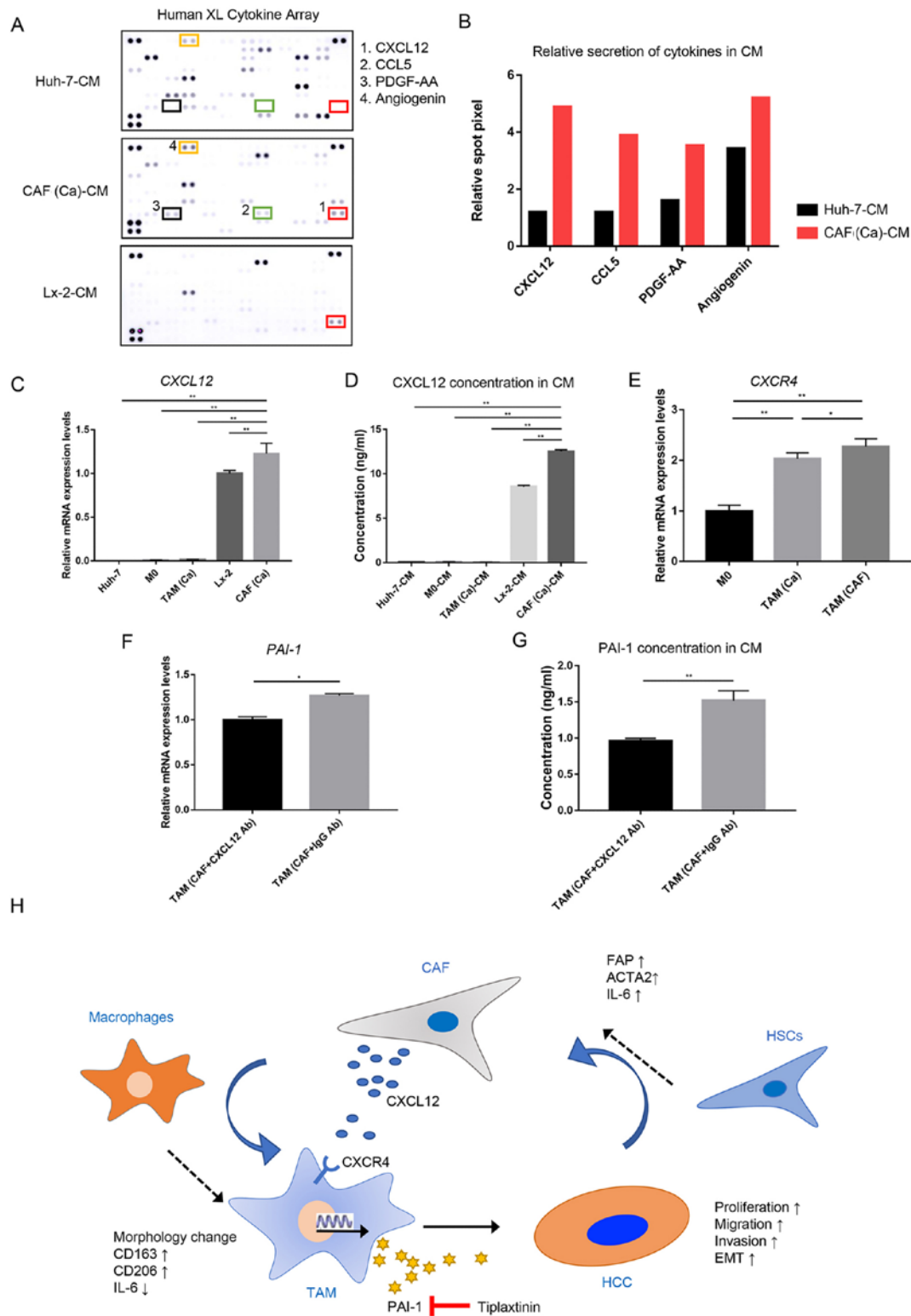


Figure 5. CAF-derived CXCL12 induces the secretion of PAI-1 in TAM(CAF). (A) Original image and (B) spot pixel value from a cytokine array to identify the different patterns of molecules in cancer-CM and CAFs-CM. *CXCL12* gene expression and its secretion were increased in CAFs compared with that in the Huh-7 and Lx-2 cells following (C) RT-qPCR and (D) ELISA. (E) *CXCR4* gene expression in M0, TAM(Ca) and TAM(CAF) was analyzed using RT-qPCR. (F) RT-qPCR and (G) ELISA results demonstrated that the gene expression level and secretion of PAI-1 were decreased in TAM(CAF) after CXCL12 neutralization in CAF-CM, respectively. (H) Schematic representation of the proposed interactions between HCC, TAMs and CAFs. * $P < 0.05$; ** $P < 0.01$. CAF, cancer-associated fibroblast; CM, conditioned medium; CCL5, C-C motif chemokine ligand 5; CXCL12, C-X-C motif chemokine ligand 12; CXCR4, C-X-C Motif chemokine receptor 4; HCC, hepatocellular carcinoma; HSCs, hepatic stellate cells; PAI-1, plasminogen activator inhibitor-1; PDGF-AA, platelet derived growth factor-AA; RT-qPCR, reverse transcription-quantitative PCR; TAM, tumor-associated macrophage; Ab, antibody.

interactions, CAFs interacted with the macrophages to induce their M2 polarization and stimulated the secretion of PAI-1 via

CXCL12. In turn, PAI-1 produced by TAM(CAF) enhanced the malignant behavior of HCC cells (Fig. 5H).

Discussion

The present study demonstrated that the HCC cells induced the differentiation of HSCs into CAFs and upregulated the mRNA expression level of CXCL12. CAF-induced macrophages exhibited a special M2 polarization phenotype and secreted PAI-1 to promote the malignant behavior of HCC cells *in vitro*. The current study also provided evidence that inhibiting the crosstalk in the TME by targeting these factors may be beneficial for HCC treatment.

CAFs are a heterogeneous population; however, HSCs with high *ACTA2* and *FAP* mRNA expression levels activated by adjacent tumor cells are considered to be the main source of CAFs in HCC (29). In the TME, infiltrated monocytes or resident macrophages are recruited by several factors, such as *CCL5* and *TGF-β*, and form a diverse spectrum of TAMs, which are the main regulators of tumor-related inflammation (30,31). TAMs are mainly divided into two different polarization types. Classically activated anti-tumorigenic M1 macrophages have pro-inflammatory characteristics and secrete IL-1 and IL-6, while alternatively activated M2 macrophages exhibit anti-inflammatory and pro-tumorigenic functions and mainly express *CD163* and *CD206* (32).

The present results demonstrated that both cancer cells and CAFs could induce the polarization of monocyte-derived macrophages into M2-polarized macrophages, which promoted the malignant characteristics of the HCC cells. Furthermore, it was identified that IL-6 concentration and expression level was significantly increased in the CAFs compared with that in the HSCs. Previous studies have reported that IL-6 could modulate the M2 macrophage polarization, and this may be a possible mechanism for CAF-CM to induce the change from the M0 macrophage phenotype into TAM (33,34). Furthermore, previous reports have revealed that, in addition to cancer cells, CAFs also induced the chemotaxis of monocytes to localize to the tumor cells via paracrine actions and induced the M2 polarization phenotype in HCC (15), PCa (35), PDAC (5), IHCC (12), breast cancer (13), OSCC (36) and ESCC (10). Similar to CAFs, macrophages display abnormal transcriptomic characteristics and functions under specific stimuli from tumor cells or stromal cells (37). Furthermore, heterogeneous TAMs secrete a variety of factors, such as IL-8, *CCL5* and VEGF, which exert various effects on cancer cells and other stromal cells, resulting in enhanced cancer cell proliferation, stemness, invasion, drug resistance and immune escape (6,32,38). The present results identified that TAM(CAF) exhibited significantly increased expression levels and secretion of a variety of factors, including PAI-1.

The paradoxical tumor-promoting abilities of PAI-1 in cancer have been a topic of increased interest. It is currently considered that the complex functional domains and various sources of PAI-1 contribute to its multiple roles in promoting cancer progression (21). While cancer cells also secrete PAI-1, the present results suggested that only TAMs treated with CAF-derived CM exhibited a significant increase in PAI-1 protein expression and secretion. However, the intensity of the expression levels of PAI-1 from western blot analysis was not as high as that in the cytokine array. We hypothesized that as a secretory protein, PAI-1 could be secreted and enriched

in the supernatant, which may lead to a higher level of PAI-1 in the supernatant.

To elucidate the mechanism in which the CAFs specifically increased PAI-1 secretion in the TAMs, the current study examined the differences in factors in the CM between the cancer cells and CAFs. It was found that CAFs secreted high amounts of CXCL12, whereas cancer cells lacked this ability. Furthermore, CXCL12 mRNA expression level was increased during the transformation of the HSCs into CAFs stimulated by cancer cells, which was consistent with findings from previous studies (39,40). In addition to the main regulators of PAI-1, such as *TNF-α* and *TGF-β* (16), CXCL12 was also found to stimulate PAI-1 expression (27). CXCL12 achieved its chemotactic effects by interacting with CXCR4. Oh *et al* (27) reported that glioma cells expressing high protein levels of CXCR4 could upregulate PAI-1 mRNA and protein expression levels under the stimulation of CXCL12, and identified that the activation of Gi protein α subunit and the ERK/MAPK signaling pathways were necessary for this process. The current results demonstrated that *CXCR4* mRNA expression level was upregulated in the TAM(CAF), and that the neutralization of CXCL12 downregulated both the mRNA expression level and the secretion of PAI-1. Taken together, it was suggested that CXCL12 interacted with CXCR4 to promote PAI-1 transcription.

The effects of PAI-1 on tumor progression are well documented. Several reports have shown that PAI-1 directly stimulated the proliferation of tumor cells by regulating cell cycle progression (41,42), and that it exerted protective effects by inhibiting Fas cell surface death receptor (Fas)/Fas ligand-mediated apoptosis (18) and inactivating caspase-3 (43). In breast cancer, PAI-1 facilitated cancer-associated adipocyte-mediated collagen remodeling and further promoted cancer metastasis by activating the PI3K/AKT/forkhead box P1 signaling pathway (44). Liu *et al* (45) reported that PAItrap3, a specific inhibitor of PAI-1, reduced the migratory and invasive abilities in breast and cervical cancer cells by inhibiting the interactions between the F-actin complex and integrins.

EMT is a process involving changes in the epithelial characteristics of cells to enhance their migratory ability (46). A decrease in E-cadherin and increase in N-cadherin mRNA and protein expression levels are typical changes in EMT (47). Our previous study revealed that lactate secreted by HCC and PDAC cells stimulated the M2 phenotypic transformation of macrophages and enhanced VEGF expression by nuclear factor erythroid 2-related factor 2 (NRF2) activation, and that M2 macrophages triggered NRF2 signaling activation in cancer cells via paracrine VEGF, thereby promoting EMT (6). Several previous studies have shown that PAI-1 contributed to cell invasion and migration by mediating EMT in colorectal cancer (19), gastric adenocarcinoma (48) and non-small cell lung cancer (49). Furthermore, the present results demonstrated that E-cadherin protein expression level was downregulated, while N-cadherin, Snail and Twist1 protein expression levels were upregulated in the Huh-7 treated with TAM(CAF), and these effects were reversed by the inhibition of PAI-1. Collectively, the current findings suggested that PAI-1 secreted from TAM(CAF) was associated with EMT in HCC cell lines.

As a selective inhibitor of PAI-1, with an IC_{50} of $2.7 \mu\text{M}$ (50), $20 \mu\text{M}$ tiplaxtinin was used to inactivate the PAI-1 in the CM in the present study. Additional experiments were also performed to confirm that tiplaxtinin, at this concentration, did not affect the proliferation of Huh-7. To date, PAI-1 inhibitors have been used in animal models of cancer and have shown effective anti-tumor activity. For example, tiplaxtinin has been reported to decrease tumor cell proliferation and vascularization in mouse models of bladder cancer and cervical cancer (51). Furthermore, SK-216 exerted an anti-tumor effect by reducing tumor size and inhibiting angiogenesis and metastasis in mice with lung carcinoma and melanoma (52). However, the short effective half-life of these inhibitors in the body has limited their clinical use, as sufficient concentrations are often difficult to achieve, particularly in the tumor area, during long-term cancer treatment (19). Therefore, anti-PAI-1 therapy in cancer treatment remains a promising but challenging strategy, and the development of more effective and safe inhibitors is required.

There are certain limitations to the present study. The mechanism of TAM polarization and the status of TAMs under immunosuppressive conditions in the TME require further investigation. Recent research has shown that the protein expression levels of PAI-1 and ACTA2 are associated with each other. For example, *in vitro* inhibition of PAI-1 downregulated the positive expression level of ACTA2 in CAFs and promoted CAF apoptosis (53). PAI-1 also increased monocyte/macrophage recruitment and M2 polarization (54). These findings suggest that the effects of PAI-1 on tumor stromal cells require further consideration.

The present study simulated the crosstalk among cancer cells, CAFs and TAMs *in vitro*, and to the best of our knowledge, reported for the first time that CAFs promoted tumor progression by inducing a special TAM phenotype. CAFs supported tumors by stimulating the M2 phenotypic transformation of macrophages and the secretion of PAI-1. PAI-1 promoted the proliferation and invasion of HCC cells by mediating EMT, and CXCL12 produced by CAFs contributed to the secretion of PAI-1 in TAMs. The current results identified CAFs as a source of soluble factors, which may regulate the phenotype of other stromal cells. Furthermore, TAMs directly promoted tumor progression via paracrine factors. Therefore, inhibiting the crosstalk between stromal cells may be a promising method for cancer treatment in HCC. Further research should be conducted to fully elucidate the complex functions of CAFs and TAMs in HCC to improve treatment for patients with HCC.

Acknowledgements

Not applicable.

Funding

This study was partly supported by the Research Program on Hepatitis from Japanese Foundation for Multidisciplinary Treatment of Cancer and the Japan Agency for Medical Research and Development (grant nos. JP19fk0210048 and JP20fk0210048), Grant-in-Aid for Scientific Research (grant nos. 20K08957 and 18K02871) and Taiho Pharmaceutical Co., Ltd.

Availability of data and materials

The datasets used and/or analyzed during the current study are available from the corresponding author on reasonable request. The cytokine datasets generated and analyzed during the current study are available in the Figshare repository (<https://doi.org/10.6084/m9.figshare.14386388.v1>).

Authors' contributions

SC, KT, YM and MS designed the experiments. SC, YS and MN performed the experiments and collected the data. SY and TI analyzed and interpreted the data. SC drafted the manuscript. YM and MS revised the paper critically for important intellectual content. SC and YM confirmed the authenticity of all the raw data. SC and YM agree to be accountable for all aspects of the work in ensuring that questions related to the accuracy or integrity of any part of the work are appropriately investigated and resolved. All the authors have read and approved the final version of the manuscript for publication.

Ethics approval and consent to participate

Not applicable.

Patient consent for publication

Not applicable.

Competing interests

The authors declare that they have no competing interests.

References

1. Metcalf KJ, Alazeh A, Werb Z and Weaver VM: Leveraging microenvironmental synthetic lethality to treat cancer. *J Clin Invest* 131: e143765, 2021.
2. Quail DF and Joyce JA: Microenvironmental regulation of tumor progression and metastasis. *Nat Med* 19: 1423-1437, 2013.
3. Bejarano L, Jordão MJ and Joyce JA: Therapeutic targeting of the tumor microenvironment. *Cancer Discov* 11: 933-959, 2021.
4. Comito G, Giannoni E, Segura CP, Barcellos-de-Souza P, Raspollini MR, Baroni G, Lanciotti M, Serni S and Chiarugi P: Cancer-associated fibroblasts and M2-polarized macrophages synergize during prostate carcinoma progression. *Oncogene* 33: 2423-2431, 2014.
5. Andersson P, Yang Y, Hosaka K, Zhang Y, Fischer C, Braun H, Liu S, Yu G, Liu S, Beyaert R, *et al*: Molecular mechanisms of IL-33-mediated stromal interactions in cancer metastasis. *JCI Insight* 3: e122375, 2018.
6. Feng R, Morine Y, Ikemoto T, Imura S, Iwahashi S, Saito Y and Shimada M: Nrf2 activation drive macrophages polarization and cancer cell epithelial-mesenchymal transition during interaction. *Cell Commun Signal* 16: 54, 2018.
7. Kang JI, Kim DH, Sung KW, Shim SM, Cha-Molstad H, Soung NK, Lee KH, Hwang J, Lee HG, Kwon YT and Kim BY: p62-Induced cancer-associated fibroblast activation via the nrf2-atf6 pathway promotes lung tumorigenesis. *Cancers (Basel)* 13: 864, 2021.
8. Torre LA, Bray F, Siegel RL, Ferlay J, Lortet-Tieulent J and Jemal A: Global cancer statistics, 2012. *CA Cancer J Clin* 65: 87-108, 2015.
9. Wu Q, Zhou LY, Lv DD, Zhu X and Tang H: Exosome-mediated communication in the tumor microenvironment contributes to hepatocellular carcinoma development and progression. *J Hematol Oncol* 12: 53, 2019.

10. Higashino N, Koma YI, Hosono M, Takase N, Okamoto M, Kodaira H, Nishio M, Shigeoka M, Kakeji Y and Yokozaki H: Fibroblast activation protein-positive fibroblasts promote tumor progression through secretion of CCL2 and interleukin-6 in esophageal squamous cell carcinoma. *Lab Invest* 99: 777-792, 2019.
11. Hashimoto O, Yoshida M, Koma YI, Yanai T, Hasegawa D, Kosaka Y, Nishimura N and Yokozaki H: Collaboration of cancer-associated fibroblasts and tumour-associated macrophages for neuroblastoma development. *J Pathol* 240: 211-223, 2016.
12. Yang X, Lin Y, Shi Y, Li B, Liu W, Yin W, Dang Y, Chu Y, Fan J and He R: Fap promotes immunosuppression by cancer-associated fibroblasts in the tumor microenvironment via STAT3-CCL2 signaling. *Cancer Res* 76: 4124-4135, 2016.
13. Allaoui R, Bergenfelz C, Mohlin S, Hagerling C, Salari K, Werb Z, Anderson RL, Ethier SP, Jirstrom K, Pahlman S, *et al*: Cancer-associated fibroblast-secreted CXCL16 attracts monocytes to promote stroma activation in triple-negative breast cancers. *Nat Commun* 7: 13050, 2016.
14. Cho H, Seo Y, Loke KM, Kim SW, Oh SM, Kim JH, Soh J, Kim HS, Lee H, Kim J, *et al*: Cancer-stimulated cdfs enhance monocyte differentiation and protumoral tam activation via il6 and GM-CSF secretion. *Clin Cancer Res* 24: 5407-5421, 2018.
15. Ji J, Eggert T, Budhu A, Forgues M, Takai A, Dang H, Ye Q, Lee JS, Kim JH, Greten TF and Wang XW: Hepatic stellate cell and monocyte interaction contributes to poor prognosis in hepatocellular carcinoma. *Hepatology* 62: 481-495, 2015.
16. Kubala MH and DeClerck YA: The plasminogen activator inhibitor-1 paradox in cancer: A mechanistic understanding. *Cancer Metastasis Rev* 38: 483-492, 2019.
17. Li SJ, Wei XH, Zhan XM, He JY, Zeng YQ, Tian XM, Yuan ST and Sun L: Adipocyte-derived leptin promotes PAI-1-mediated breast cancer metastasis in a STAT3/miR-34a dependent manner. *Cancers (Basel)* 12: 3864, 2020.
18. Mashiko S, Kitatani K, Toyoshima M, Ichimura A, Dan T, Usui T, Ishibashi M, Shigeta S, Nagase S, Miyata T and Yaegashi N: Inhibition of plasminogen activator inhibitor-1 is a potential therapeutic strategy in ovarian cancer. *Cancer Biol Ther* 16: 253-260, 2015.
19. Muñoz-Galván S, Rivero M, Peinado-Serrano J, Martínez-Pérez J, Fernández-Fernández MC, Ortiz MJ, García-Heredia JM and Carnero A: PAI1 is a marker of bad prognosis in rectal cancer but predicts a better response to treatment with PIM inhibitor AZD1208. *Cells* 9: 1071, 2020.
20. Fang H, Placencio VR and DeClerck YA: Protumorigenic activity of plasminogen activator inhibitor-1 through an antiapoptotic function. *J Natl Cancer Inst* 104: 1470-1484, 2012.
21. Placencio VR and DeClerck YA: Plasminogen activator inhibitor-1 in cancer: Rationale and insight for future therapeutic testing. *Cancer Res* 75: 2969-2974, 2015.
22. Jin Y, Liang ZY, Zhou WX and Zhou L: Expression, clinicopathologic and prognostic significance of plasminogen activator inhibitor 1 in hepatocellular carcinoma. *Cancer Biomark* 27: 285-293, 2020.
23. Livak KJ and Schmittgen TD: Analysis of relative gene expression data using real-time quantitative PCR and the 2(-Delta Delta C(T)) method. *Methods* 25: 402-408, 2001.
24. Zhang J, Zhang Q, Lou Y, Fu Q, Chen Q, Wei T, Yang JQ, Tang J, Wang J, Chen Y, *et al*: Hypoxia-inducible factor-1 α /interleukin-1 β signaling enhances hepatoma epithelial-mesenchymal transition through macrophages in a hypoxic-inflammatory microenvironment. *Hepatology* 67: 1872-1889, 2018.
25. Dahlem C, Siow WX, Lopatniuk M, Tse WK, Kessler SM, Kirsch SH, Hoppstädter J, Vollmar AM, Müller R, Luzhetskyy A, *et al*: Thiologamide A, a new anti-proliferative anti-tumor agent, modulates macrophage polarization and metabolism. *Cancers (Basel)* 12: 1288, 2020.
26. Che Y, Wang JN, Li Y, Lu ZL, Huang JB, Sun SG, Mao SS, Lei YY, Zang RC, Sun N and He J: Cisplatin-activated PAI-1 secretion in the cancer-associated fibroblasts with paracrine effects promoting esophageal squamous cell carcinoma progression and causing chemoresistance. *Cell Death Dis* 9: 759, 2018.
27. Oh JW, Olman M and Benveniste EN: CXCL12-mediated induction of plasminogen activator inhibitor-1 expression in human CXCR4 positive astroglia cells. *Biol Pharm Bull* 32: 573-577, 2009.
28. Phillips RJ, Burdick MD, Lutz M, Belperio JA, Keane MP and Strieter RM: The stromal derived factor-1/CXCL12-CXC chemokine receptor 4 biological axis in non-small cell lung cancer metastases. *Am J Respir Crit Care Med* 167: 1676-1686, 2003.
29. Yin ZL, Dong CY, Jiang KQ, Xu Z, Li R, Guo K, Shao SJ and Wang L: Heterogeneity of cancer-associated fibroblasts and roles in the progression, prognosis, and therapy of hepatocellular carcinoma. *J Hematol Oncol* 12: 101, 2019.
30. Pham K, Huynh D, Le L, Delitto D, Yang L, Huang J, Kang Y, Steinberg MB, Li J, Zhang L, *et al*: E-cigarette promotes breast carcinoma progression and lung metastasis: Macrophage-tumor cells crosstalk and the role of CCL5 and VCAM-1. *Cancer Lett* 491: 132-145, 2020.
31. Yan W, Liu X, Ma H, Zhang H, Song X, Gao L, Liang X and Ma C: Tim-3 fosters HCC development by enhancing TGF- β -mediated alternative activation of macrophages. *Gut* 64: 1593-1604, 2015.
32. Franklin RA, Liao W, Sarkar A, Kim MV, Bivona MR, Liu K, Pamer EG and Li MO: The cellular and molecular origin of tumor-associated macrophages. *Science* 344: 921-925, 2014.
33. Yin Z, Ma TT, Lin Y, Lu X, Zhang CZ, Chen S and Jian ZX: IL-6/STAT3 pathway intermediates M1/M2 macrophage polarization during the development of hepatocellular carcinoma. *J Cell Biochem* 119: 9419-9432, 2018.
34. Wang Q, He Z, Huang M, Liu T, Wang Y, Xu H, Duan H, Ma P, Zhang L, Zamvil SS, *et al*: Vascular niche IL-6 induces alternative macrophage activation in glioblastoma through HIF-2 α . *Nat Commun* 9: 559, 2018.
35. Augsten M, Sjöberg E, Frings O, Vorrink SU, Frijhoff J, Olsson E, Borg A and Östman A: Cancer-associated fibroblasts expressing CXCL14 rely upon NOS1-derived nitric oxide signaling for their tumor-supporting properties. *Cancer Res* 74: 2999-3010, 2014.
36. Li X, Bu WH, Meng L, Liu XC, Wang SS, Jiang LM, Ren MS, Fan Y and Sun HC: CXCL12/CXCR4 pathway orchestrates CSC-like properties by CAF recruited tumor associated macrophage in OSCC. *Exp Cell Res* 378: 131-138, 2019.
37. Murray PJ: Macrophage polarization. *Annu Rev Physiol* 79: 541-566, 2017.
38. Huang CP, Liu LX and Shyr CR: Tumor-associated macrophages facilitate bladder cancer progression by increasing cell growth, migration, invasion and cytokine expression. *Anticancer Res* 40: 2715-2724, 2020.
39. Feig C, Jones JO, Kraman M, Wells RJ, Deonarine A, Chan DS, Connell CM, Roberts EW, Zhao Q, Caballero OL, *et al*: Targeting CXCL12 from FAP-expressing carcinoma-associated fibroblasts synergizes with anti-PD-L1 immunotherapy in pancreatic cancer. *Proc Natl Acad Sci U S A* 110: 20212-20217, 2013.
40. Tan HX, Gong WZ, Zhou K, Xiao ZG, Hou FT, Huang T, Zhang L, Dong HY, Zhang WL, Liu Y and Huang ZC: CXCR4/TGF- β 1 mediated hepatic stellate cells differentiation into carcinoma-associated fibroblasts and promoted liver metastasis of colon cancer. *Cancer Biol Ther* 21: 258-268, 2020.
41. Giacoia EG, Miyake M, Lawton A, Goodison S and Rosser CJ: PAI-1 leads to G1-phase cell-cycle progression through cyclin D3/cdk4/6 upregulation. *Mol Cancer Res* 12: 322-334, 2014.
42. Liu SL, Wu XS, Li FN, Yao WY, Wu ZY, Dong P, Wang XF and Gong W: ERR α promotes pancreatic cancer progression by enhancing the transcription of PAI1 and activating the MEK/ERK pathway. *Am J Cancer Res* 10: 3622-3643, 2020.
43. Chen Y, Kelm RJ Jr, Budd RC, Sobel BE and Schneider DJ: Inhibition of apoptosis and caspase-3 in vascular smooth muscle cells by plasminogen activator inhibitor type-1. *J Cell Biochem* 92: 178-188, 2004.
44. Wei X, Li S, He J, Du H, Liu Y, Yu W, Hu H, Han L, Wang C, Li H, *et al*: Tumor-secreted PAI-1 promotes breast cancer metastasis via the induction of adipocyte-derived collagen remodeling. *Cell Commun Signal* 17: 58, 2019.
45. Liu J, Chen Z, Huang M, Tang S, Wang Q, Hu P, Gupta P, Ashby CR Jr, Chen ZS and Zhang L: Plasminogen activator inhibitor (PAI) trap3, an exocellular peptide inhibitor of PAI-1, attenuates the rearrangement of F-actin and migration of cancer cells. *Exp Cell Res* 391: 111987, 2020.
46. Chen S, Kang X, Liu G, Zhang B, Hu X and Feng Y: α 7-Nicotinic acetylcholine receptor promotes cholangiocarcinoma progression and epithelial-mesenchymal transition process. *Dig Dis Sci* 64: 2843-2853, 2019.
47. Pal M, Bhattacharya S, Kalyan G and Hazra S: Cadherin profiling for therapeutic interventions in epithelial mesenchymal transition (EMT) and tumorigenesis. *Exp Cell Res* 368: 137-146, 2018.
48. Yang JD, Ma L and Zhu Z: SERPINE1 as a cancer-promoting gene in gastric adenocarcinoma: Facilitates tumour cell proliferation, migration, and invasion by regulating EMT. *J Chemother* 31: 408-418, 2019.

49. Lin X, Lin BW, Chen XL, Zhang BL, Xiao XJ, Shi JS, Lin JD and Chen X: PAI-1/PLAS3/Stat3/miR-34a forms a positive feedback loop to promote EMT-mediated metastasis through Stat3 signaling in non-small cell lung cancer. *Biochem Biophys Res Commun* 493: 1464-1470, 2017.
50. Hennen JK, Morgan GA, Swillo RE, Antrilli TM, Mugford C, Vlasuk GP, Gardell SJ and Crandall DL: Effect of tiplaxtinin (PAI-039), an orally bioavailable PAI-1 antagonist, in a rat model of thrombosis. *J Thromb Haemost* 6:1558-1564, 2008.
51. Gomes-Giacoaia E, Miyake M, Goodison S and Rosser CJ: Targeting plasminogen activator inhibitor-1 inhibits angiogenesis and tumor growth in a human cancer xenograft model. *Mol Cancer Ther* 12: 2697-2708, 2013.
52. Masuda T, Hattori N, Senoo T, Akita S, Ishikawa N, Fujitaka K, Haruta Y, Murai H and Kohno N: SK-216, an inhibitor of plasminogen activator inhibitor-1, limits tumor progression and angiogenesis. *Mol Cancer Ther* 12: 2378-2388, 2013.
53. Masuda T, Nakashima T, Namba M, Yamaguchi K, Sakamoto S, Horimasu Y, Miyamoto S, Iwamoto H, Fujitaka K, Miyata Y, *et al*: Inhibition of PAI-1 limits chemotherapy resistance in lung cancer through suppressing myofibroblast characteristics of cancer-associated fibroblasts. *J Cell Mol Med* 23: 2984-2994, 2019.
54. Kubala MH, Punj V, Placencio-Hickok VR, Fang H, Fernandez GE, Sposto R and DeClerck YA: Plasminogen activator inhibitor-1 promotes the recruitment and polarization of macrophages in cancer. *Cell Rep* 25: 2177-2191, 2018.



This work is licensed under a Creative Commons Attribution-NonCommercial-NoDerivatives 4.0 International (CC BY-NC-ND 4.0) License.